Full Paper

Amperometric Glucose Biosensing of Gold Nanoparticles and Carbon Nanotube Multilayer Membranes

Ying Liu, Shuo Wu, Huangxian Ju, Li Xu*

MOE Key Laboratory of Analytical Chemistry for Life Science, School of Chemistry and Chemical Engineering, Nanjing University, Nanjing 210093, P. R. China
*e-mail: hxju@nju.edu.cn

Received: November 17, 2006
Accepted: January 26, 2007

Abstract
A novel multilayer gold nanoparticles/multiwalled carbon nanotubes/glucose oxidase membrane was prepared by electrostatic assembly using positively charged poly(dimethyldiallylammonium chloride) to connect them layer by layer. The modification process and membrane structures were characterized by atomic force microscopy, scanning electron microscopy and electrochemical methods. This membrane showed excellent electrocatalytic character for glucose biosensing at a relatively low potential (−0.2 V). The K_m value of the immobilized glucose oxidase was 10.6 mM. This resulting sensor could detect glucose up to 9.0 mM with a detection limit of 128 μM and showed excellent analytical performance.

Keywords: Amperometric biosensors, Multilayer, Multiwalled carbon nanotube, Gold nanoparticle, Glucose

DOI: 10.1002/elan.200603814

1. Introduction

Gold nanoparticles (GNP) possess excellent catalytic activity due to their high surface area-to-volume ratios and good interface-dominated properties [1, 2], which offers a friendly environment to immobilize protein molecules [3]. In addition, the GNP can act as fine antennae to transfer electron at the electrode/solution interface, thus is helpful for producing direct electrochemistry of proteins such as glucose oxidase, cytochrome c, myoglobin [4] and hemoglobin [5], and effective catalysis to the oxygen reduction [6, 7]. Recently, several multilayer membranes with a layer-by-layer structure of GNP and other polyelectrolytes have been studied due to the controllable character of interfaces, including cationic poly(L-lysine) and mercaptosuccinic acid stabilized gold nanoparticles [8], and glucose oxidase/poly(diallydimethylammonium chloride)(PDDA)/GNP multilayer films [9]. The layer-by-layer structure improved the permeability of the multilayer films for infiltration and effective contact of glucose with the inside layer of enzyme.

Carbon nanotubes (CNT) have won great interest because of their unique electronic [10] and mechanical [11] properties combined with chemical stability. Owing to the atomic structure, CNT can behave electrically as a metal or semiconductor [12]. Recent studies have showed the application of CNT in various fields, for example, the detection of DNA hybridization [13, 14], the direct electron transfer of proteins such as GOD [15] and cytochrome c [16], and the electrocatalysis to reduction of oxygen [17–19] and hydrogen peroxide [19]. Recently, the aligned CNT worked as nanoelectrodes has been studied for glucose detection through its excellent catalysis to reduction of hydrogen peroxide [20]. Of course, a majority of applications concerns the detection of some molecules which participated in the life process, including dopamine and ascorbic acid [21], cholesterol [22], and glucose [20, 23].

The glucose biosensors are generally based on the detection of the oxidation signal of hydrogen peroxide or the reduction signal of dissolved oxygen, which is produced or consumed in the oxidation process of β-D-glucose to D-glucono-δ-lactone catalyzed by GOD, respectively. Most of glucose biosensors detect glucose by the first method with the excellent oxidation signal [24–26]. However, this method is performed at a positive potential, thus needs a polymer membrane (e.g., Nafion) to avoid the interference of ascorbic acid (AA) and uric acid (UA), decreasing the sensitivity and complicating the modification process. The second method generally encounters a shortcoming of low upper limit of the linear range [27, 28]. To overcome this defect, several methods, including utilizing an oxygen-sensitive optode membrane for optical biosensor [29], a mass-transport limiting film to tailor the flux of glucose and oxygen [30, 31] and a fast redox mediator such as ferrocene instead of oxygen [32], have been developed. The mass-transport limiting film suffers from low sensitivity and the use of redox mediator results in other problems such as less stability or complicated procedures. In comparison, the multilayer structure of GNP and MWNTs prepared with a simple modification process in this work not only increases the electrocatalysis of oxygen reduction, but also prompts the permeability of oxygen, which increases the oxygen content around the electrode surface, thus extends the upper

limit of the linear range and improves the sensitivity of glucose biosensing.

GNP can be attached to the surface of CNT in solution to form a nanohybrid [33] for development of genosensors [34]. Kim and Sigmund [35] developed a CNT/GNP composite via electrostatic assembly in the presence of polyelectrolytes. Here, aiming to detect glucose via oxygen consumption, we prepared a multilayer membrane composed of GNP, MWNTs, and GOD by electrostatic assembly using positively charged poly(dimethyldiallylammonium chloride) (PDDA) to connect them layer by layer, making use of the advantages of GNP and MWNTs multilayer membrane to electrocatalyze oxygen reduction, increase the electroactive surface areas, and prompt the permeability of oxygen. Compared with former glucose sensors based on MWNTs and GOD modified electrodes [27, 36], this work decreased the reduction overpotential of dissolved oxygen, could thus exclude the interference from some electrochemically reducible compounds. Furthermore, different from those based on the oxidation of hydrogen peroxide [9, 37], it also excluded the interference from electrochemically oxidizable compounds such as ascorbic acid and uric acid.

2. Experimental

2.1. Chemicals and Materials

GOD (type II-S, from *Aspergillus niger*; 39.8 U/mg), cysteamine ($NH_2CH_2CH_2SH$) were purchased from Sigma. PDDA ($M_W = 100{,}000 - 200{,}000$ g/mol) in 20% aqueous solution was purchased from Aldrich. MWNTs (>95%, 40 – 60 nm diameter) were purchased from Shenzhen Nanotech Port Ltd. Co (Shenzhen, China). All other chemicals were of analytical grade and were used as received. Twice-distilled water was used throughout the experiments.

Citrate stabilized GNP solution with the GNP particle size of about 20 nm was prepared according to the literature [38] and stored in brown glass bottles at 4 °C and kept stable for about 1 month.

2.2. Preparation of GNP/MWNTs/GOD Multilayer Membrane

MWNTs were refluxed in 30% nitric acid at 100 °C for about 12 hours, filtered, washed with double-distilled water until the filtrate became neutral, and finally dried under vacuum. Such a procedure shortened the nanotubes, produced carboxylic acid groups mainly on the open ends as well as the sidewalls, thus introduced negative charges to MWNTs and improved the their dispersion in water.

1.0 mg acid-pretreated MWNTs were dispersed in 1.0 mL water with an ultrasonic bath for 10 min, giving a black suspension that was stable for 2 weeks. Gold disc electrodes (CH Instruments Inc., USA, 2.0 mm in diameter) were abraded with fine silicon carbide paper and polished carefully with 0.3- and 0.05-μm alumina slurry, and then sonicated in water and absolute ethanol. The cysteamine self-assembled monolayer (Au/Cys) was prepared by immersing the cleaned gold electrode into 0.1 M cysteamine solution for 5 hours at 4 °C and then washed with distilled water. This electrode was then modified by a 12 μL drop of GNP solution and dried in air at 4 °C. After washing with distilled water to remove the excess of assembly materials, the electrode was immersed in 1% PDDA + 0.5 M NaCl aqueous solution for approximately 30 minutes to adsorb PDDA on GNP via electrostatic action. The addition of 0.5 M NaCl to PDDA solution was reported to result in a uniform modified layer growth since the presence of salts clearly increased the amount of polyelectrolyte deposition [39]. After washed and dried, 6 μL 1.0 mg/mL MWNTs suspension solution was dripped on the surface and dried in air, producing a multilayer membrane containing both GNP and MWNTs.

The enzyme solution was prepared by dissolving 6 mg GOD in 1 mL pH 7.0 phosphate buffer solution (PBS). After the GNP/MWNTs modified electrode was immersed in 1% PDDA + 0.5 M NaCl aqueous solution for 30 minutes and washed with distilled water, a 1 μL drop of the enzyme solution was cast on the electrode and dried at 4 °C. After washed with distilled water, the GNP/MWNTs/GOD modified electrode was prepared and stored at 4 °C.

2.3. Electrochemical Measurements and AFM, SEM Characterization

Amperometric and cyclic voltammetric experiments were performed on a CHI 660B Electrochemical Workstation (CH Instruments Inc., USA). All experiments were carried out using a conventional three-electrode system with the modified gold disc electrode as working, a platinum foil as auxiliary, and a saturated calomel electrode as reference electrodes.

The atomic force microscopic (AFM) images of gold slides after the deposition of GNP, GNP/MWNTs, and GNP/MWNTs/GOD were obtained in air using a SPI 3800 probe station (Seiko Instruments Inc., Japan) with a Si cantilever operated in tapping mode. The gold slides were modified in the same way as that of electrodes.

The morphologies of glass slides after the deposition of MWNTs, GNP/MWNTs were studied on LEO-1530 scanning electron microscope (SEM, LEO Electron Microscopy Inc., Cambridge, UK). Glass slides were negatively charged using the same method above, and immersed in 1% PDDA + 0.5 M NaCl aqueous solution to introduce positive charges on them, then modified in the same way as that of cysteamine modified gold electrodes.

3. Results and Discussion

3.1. Assembly and Characterization of Multilayer Membrane

GOD is negatively charged in pH 7.0 PBS considering its isoelectric point (p*I*) of 4.2, which makes it suitable to

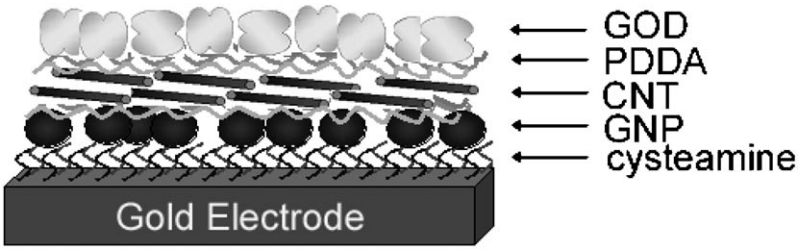

Fig. 1. Schematic structure of the multilayer membrane.

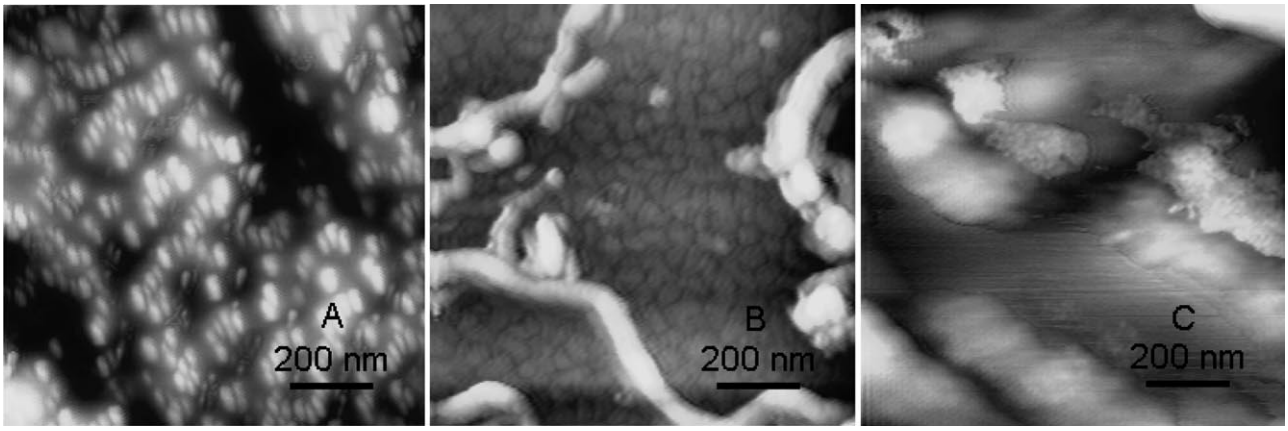

Fig. 2. AFM plots of GNP (A), GNP-PDDA-MWNTs (B), and GNP-PDDA-MWNTs-PDDA-GOD (C) membrane.

construct multilayer films via electrostatic assembly. As shown in Figure 1, initially, a layer of cysteamine was self-assembled onto the gold electrode surface via a covalent bond between −SH and Au, then similarly, the exposed $-NH_2$ of cysteamine connected citrate stabilized GNP. The positively charged PDDA layer acted as a joining to connect firstly the negatively charged MWNTs to the negatively charged GNP layer and then negatively charged GOD to the MWNTs layer. Thus a stable GNP/MWNTs/GOD multilayer membrane could be obtained on the cysteamine modified electrode.

Figure 2 shows the top AFM morphologies of a series of gold slides after modification of GNP, GNP/MWNTs or GNP/MWNTs/GOD multilayer films. After the modification of GNP, a homogeneously distributed film with bright dots about 20 nm in size was obtained (Fig. 2A), indicating the assembly of gold nanoparticles. In Figure 2B, a typical AFM image of MWNTs with about 50 nm in diameter was observed, indicating the good dispersion of MWNTs on the modification layers of GNP and PDDA. At the same time, the nanoparticles were not observed and the AFM image showed a uniform porous background, indicating the PDDA layer covered very homogenously on the layer of GNP. GNP/MWNTs/GOD multilayer film exhibited a surface with cotton-like nanoparticles, indicative of the adsorption and aggregation of GOD on PDDA layer (Fig. 2C).

The SEM images of both the MWNTs and the GNP/MWNTs modified glass slides were shown in Figure 3, respectively. The presence of GNP layer held more MWNTs on the surface, which increased the electroactive surface area as well as the electrocatalysis to the reduction of dissolved oxygen, besides, it formed a well-distributed layer compared with the electrode modified by MWNTs alone. Furthermore, GNP/MWNTs multilayer membrane exhibited a porous structure due to the difference in rigidity of the GNP, PDDA, and MWNTs layers, thus increased oxygen content around the electrode surface, and led to a high sensitivity in biosensing application.

3.2. Electrochemical Characteristic of GNP/MWNTs Multilayer Membrane

Figure 4 represents the cyclic voltammograms of the bare and three different modified electrodes in 25 mM KCl solution containing 2.5 mM $[Fe(CN)_6]^{3-}$ at 100 mV/s. The well-defined oxidation and reduction peaks were due to the electrode reaction of $[Fe(CN)_6]^{3-/4-}$ redox couple. The reduction and oxidation peak currents increased upon the modification process, indicating larger accessible surface or more electroactive surface areas were formed. According to the Randles – Sevcik equation [40], the electroactive surface area of GNP/MWNTs modified electrode for $[Fe(CN)_6]^{3-/4-}$ redox couple was about 1.4 times that of the MWNTs modified electrode. Compared with both bare and GNP modified electrodes, the cyclic voltammograms of both MWNTs and GNP/MWNTs multilayer films modified electrodes showed larger current at potentials more neg-

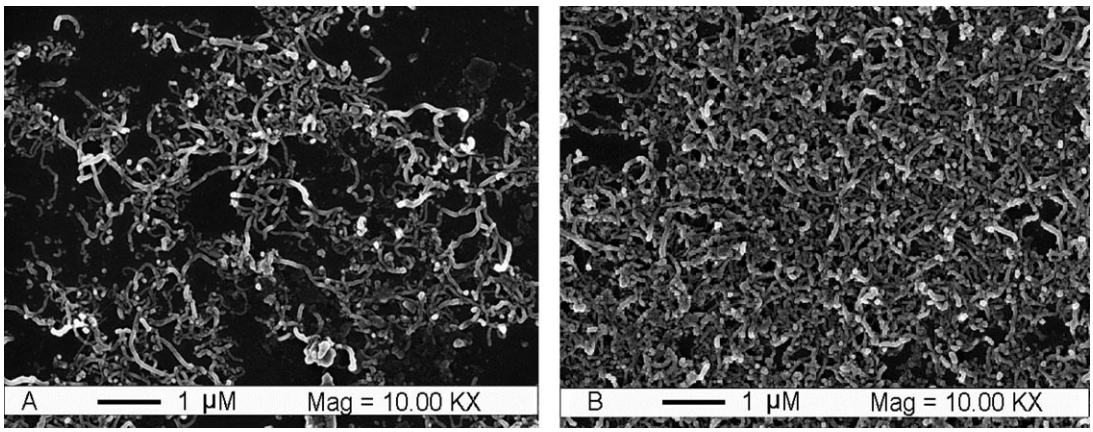

Fig. 3. SEM images of MWNTs (A) and GNP-PDDA-MWNTs (B) membrane.

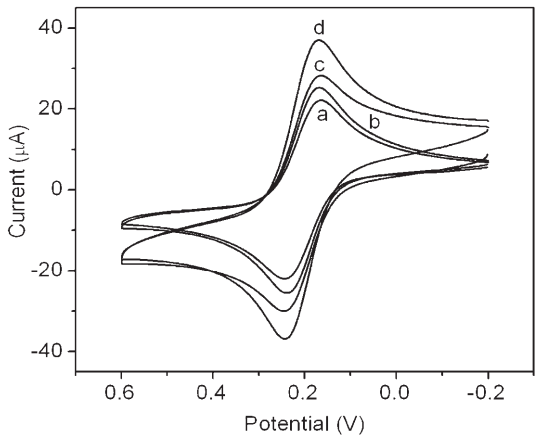

Fig. 4. Cyclic voltammograms of 2.5 mM $K_3Fe(CN)_6$ in 25 mM KCl at bare (a), GNP modified (b), MWNTs modified (c), and GNP/MWNTs modified gold electrodes (d) at 100 mV/s.

ative than the reduction peak potential of $[Fe(CN)_6]^{3-/4-}$ redox couple due to the redox reaction of MWNTs, which would be discussed in the following section.

3.3. Electrocatalysis of GNP/MWNTs Multilayer Membrane Toward Oxygen Reduction

The GNP/MWNTs modified electrode showed a pair of redox peaks in nitrogen saturated PBS (curve a, inset in Fig. 5A), which was attributed to the oxidation and reduction of MWNT-COOH. When the solution was saturated with oxygen by bubbling with oxygen for 10 minutes, a cyclic voltammogram similar to general electrocatalytic process with a great increase of the reduction peak and a decrease of the oxidation peak was observed (curve b, inset in Fig. 5A). Thus the immobilized MWNTs possessed good electrocatalytic ability to the reduction of dissolved oxygen.

The electrocatalytic ability depended on the multilayer properties. As shown in Figure 5A, the cyclic voltammograms of different modified electrodes gave different electrocatalytic currents. At the bare gold electrode the reduction peak of oxygen to produce hydrogen peroxide in neutral aqueous media occurred at -0.4 V at 100 mV/s (curve a, Fig. 5A). No obvious potential change of dissolved oxygen reduction was observed at the cysteamine self-assembly monolayer modified electrode, while the peak current decreased slightly. However, the reduction overpotential decreased greatly upon the formation of GNP layer on the cysteamine self-assembly monolayer. The reduction peak of dissolved oxygen occurred at -0.221 V and the peak current increased (curve b, Fig. 5A), indicating that GNP effectively catalyzed oxygen reduction, which was in accord with the report previously [6, 7]. The presence of CNT could also catalyze the reduction of dissolved oxygen [16, 36, 41]. The MWNTs modified electrode showed a reduction peak potential of -0.278 V with a larger peak current than that at the bare electrode at 100 mV/s (curve c, Fig. 5A). Particularly, the GNP/MWNTs multilayer films modified electrode showed greater peak current of dissolved oxygen than both GNP and MWNTs film modified electrodes (curve d, Fig. 5A), which was due to the larger electroactive surface area of the multilayer membrane. It was noted that the reduction peak of dissolved oxygen occurred at -0.190 V at 100 mV/s, more positive than those at both the GNP and MWNTs film modified electrodes, indicating the multilayer membrane had better electrocatalytic ability due to the coordinated action of GNP and MWNTs films, which led to better sensitivity for biosensing of both dissolved oxygen and biomolecules based on their oxidation by dissolved oxygen in enzymatic reactions.

The cyclic voltammograms of dissolved oxygen in pH 7.0 PBS at GNP/MWNTs multilayer films modified electrode at the scan rates from 20 to 600 mV/s were shown in Figure 5B. The electrocatalytic peak current was proportional to the square root of scan rate (curve b, inset in Fig. 5B), indicating a fast electrocatalytic process and that the diffusion of dissolved oxygen controlled the whole electrode process. Besides, the linear slope at GNP/MWNTs multilayer films modified electrode was 1.54 μA/(mV/s) (curve b, inset in Fig. 5B), twice larger than 0.65 μA/(mV/s) (curve a, inset in Fig. 5B) at MWNTs film modified electrode due to the

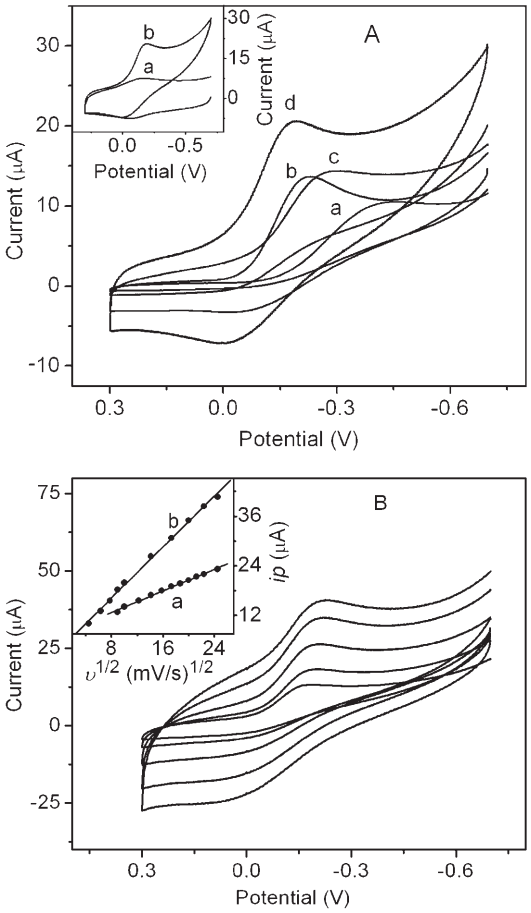

Fig. 5. Cyclic voltammograms of A) oxygen saturated 0.2 M pH 7.0 PBS at bare (a), GNP modified (b), MWNTs modified (c), and GNP/MWNTs modified (d) gold electrodes at 100 mV/s and B) GNP/CNT modified electrode in oxygen saturated 0.2 M pH 7.0 PBS at 40, 80, 200, 400, and 600 mV/s (from inner to outer). Inset in (A): cyclic volatmmograms of GNP/MWNTs modified electrode in 0.2 M pH 7.0 PBS in the absence (a) and presence (b) of saturated oxygen. Inset in (B): plots of reduction peak currents vs. $\nu^{1/2}$ at MWNTs modified (a) and GNP/MWNTs modified (b) electrodes.

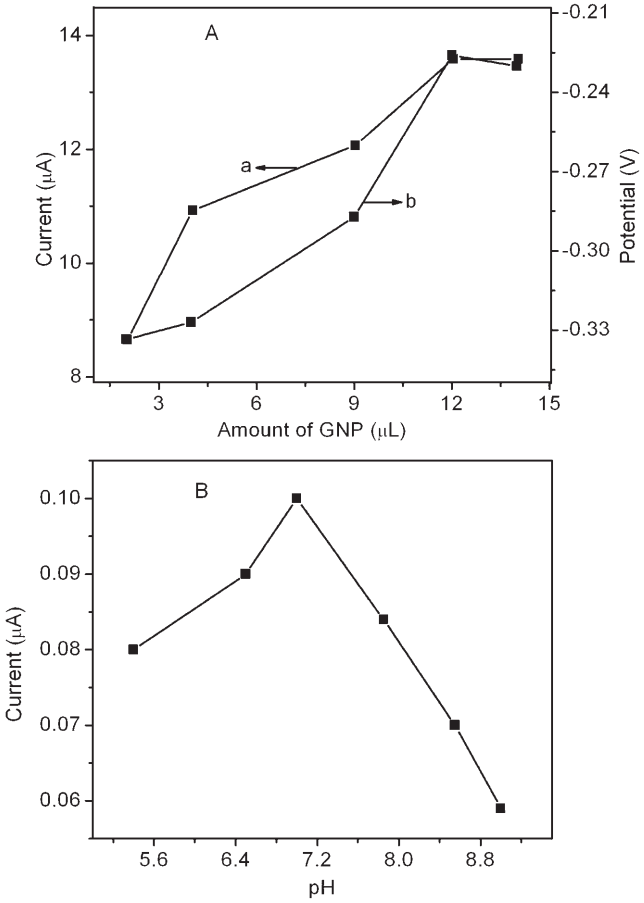

Fig. 6. Dependence of reduction peak current (a) and peak potential (b) of saturated oxygen at GNP modified electrode on the amount of GNP in 0.2 M pH 7.0 PBS (A) and influence of the solution pH on the response of GNP/MWNTs/GOD modified gold electrode to 0.5 mM glucose (B).

better electrocatalytic ability and larger active surface area of GNP/MWNTs modified electrode [41].

3.4. Effect of GNP Layer on Electrocatalytic Ability

With the increasing of GNP amount assembled on the cysteamine self-assembly monolayer, the reduction peak current of dissolved oxygen at GNP/MWNTs multilayer films modified electrode increased and reached a maximum value at the volume of 12 μL GNP solution, while the peak potential moved to more positive potential until 12 μL GNP solution was used for preparation of GNP/MWNTs multilayer films (Fig. 6A). If the GNP amount continued to increase, the response of dissolved oxygen began to fall. Thus, 12 μL GNP solution was enough to form a GNP layer on cysteamine self-assembly monolayer for further preparation of an excellent GNP/MWNTs multilayer membrane.

3.5. Performance of GNP/MWNTs/GOD Multilayer Membrane as a Glucose Biosensor

The oxidation of glucose catalyzed by glucose oxidase can consume dissolved oxygen to produce hydrogen peroxide. Using glucose and glucose oxidase (GOD) as models of biomolecules and oxidases to examine the biosensing applications of the GNP/MWNTs multilayer films, GOD was further assembled on the multilayer films with PDDA as a joining to form a GNP/MWNTs/GOD modified electrode. The saturated concentration of dissolved oxygen in water was 2.6×10^{-4} mol/L [42], and its reduction at this electrode occurred at 0.002 V with a reduction peak potential of -0.197 V (Fig. 7A). At the same concentration the reduction of hydrogen peroxide began at -0.201 V (Fig. 7B). Upon addition of 15 mM glucose to the solution, the reduction peak current of dissolved oxygen at the GNP/MWNTs/GOD modified electrode decreased due to the

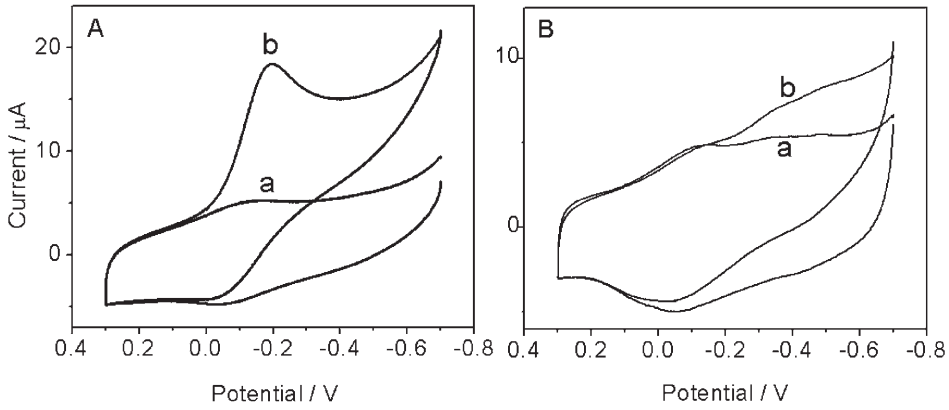

Fig. 7. Cyclic voltammograms of A) 0.2 M pH 7.0 PBS saturated with nitrogen (a) and oxygen (b) and (B) 0.2 M pH 7.0 PBS saturated with nitrogen (a) and containing 2.6×10^{-4} mol/L H_2O_2 (b) at GNP/MWNTs/GOD modified electrode at 100 mV/s.

consumption of dissolved oxygen (not shown). Based on this process, the concentration of glucose could be detected quantitatively at -0.200 V, at which the formation of hydrogen peroxide did not affect the response of dissolved oxygen.

The effect of the pH value of detection solution on the amperometric response of the GNP/MWNTs/GOD modified electrode to the injection of 0.5 mM glucose at -0.2 V was shown in Figure 6B. The maximum response was observed at pH 7.0, which was near the physiological environment. Either the strong acidic solution or alkaline solution would decrease the bioactivity of the enzyme. Thus the proposed biosensor was practicable to detect glucose levels in real samples at neutral pH value.

Figure 8 shows a typical current–time response for successive additions of glucose into 1.0 mL pH 7.0 PBS with the amounts labeled in the Figure. A sharp decrease of current was observed upon addition of glucose, and the response reached 95% steady state value within 10 s. The sensitivity of the GNP/MWNTs/GOD modified electrode was about 7.3 μA/mM cm^2, which was higher than those of 5.6 μA/mM cm^2 at {PDDA-MWNTs/ GOD}$_5$ membrane based glucose biosensors [36] and 3.9 μA/ mM cm^2 at {PDDA/GNP /PDDA/GOD}n membrane based glucose biosensors [9], indicating that the coexistence of GNP and MWNTs effectively improved the sensitivity of glucose biosensors.

The detection limit of the GNP/MWNTs/GOD based glucose biosensor was estimated to be 128 μM at a signal-to-noise ratio of 3. Its linear calibration range extended up to 9.0 mM ($R = 0.994, n = 9$) (inset A in Fig. 8), which was higher than those of 5.0 and 2.0 mM reported for previous oxygen-sensitive glucose biosensors [36, 43, 44], respectively. The extended linear range was due to the presence of both GNP and MWNTs. The multilayer structure of GNP/MWNTs/GOD increased the oxygen content around the electrode surface as well as its permeability through the multilayer film. These advantages of the GNP/MWNTs/GOD modified electrode made it practicable to detect the normal glucose concentration in blood serum of around 4.6 mM.

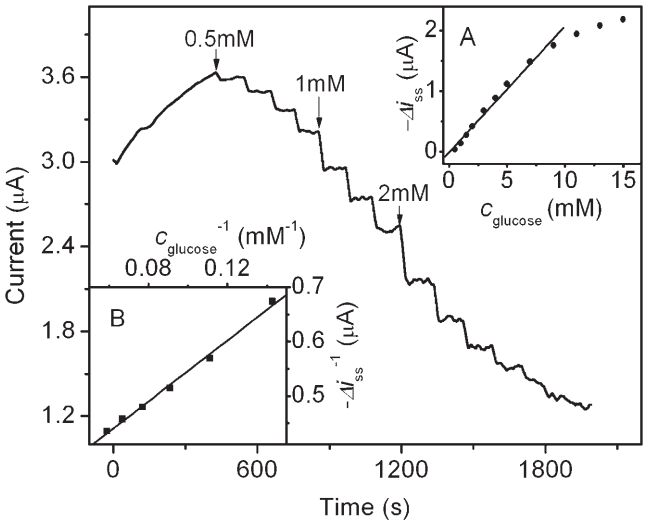

Fig. 8. Amperometric response of GNP/MWNTs/GOD modified gold electrodes at an applied potential of -0.2 V to successive additions of glucose in a stirred 0.2 M pH 7.0 PBS saturated with oxygen. Insets: calibration curves of GNP/MWNTs/GOD modified gold electrodes (A) and plot of Lineweaver–Burk equation of GNP/MWNTs/GOD modified electrode (B).

The proposed glucose biosensor exhibited a typical characteristic of Michaelis–Menten kinetics at high glucose concentrations. With the Lineweaver–Burk equation the Michaelis–Menten constant (K_m) was evaluated from the inset B in Figure 8 to be 10.5 mM, which was near to the usual K_m value and much lower than that of 22 ± 2 mM reported previously [45, 46]. This result showed that the proposed biosensor provided the GOD higher affinity to glucose than in the reported membrane [45, 46].

When a detection potential of -0.2 V was employed, neither the injection of ascorbic acid nor uric acid caused any interference to the current response (not shown). In contrast, the interference of both ascorbic acid and uric acid were obvious when the detection potential of 0.7 V was used for other glucose biosensors. The response of interfering

species even exceeded the response of the same amount of glucose. Thus, the use of a low detection potential avoided the influence of common interference. This was another advantage of the proposed biosensor.

The reproducibility and storage stability of the biosensor were examined. The relative standard deviation (*RSD*) of the biosensor response to 1.0 mM glucose was 1.5% for 3 successive measurements. The *RSD* for detection of 1.0 mM glucose with three sensors prepared independently under the same conditions was 4.6%. When the biosensor was stored in dry at 4 °C and measured every day, it retained about 83% of its original sensitivity after 3 weeks. On the other hand, the response to dissolved oxygen had no apparent decrease, indicating that the multilayer was stable.

4. Conclusions

This work constructs a GNP/MWNTs/GOD multilayer membrane, studies its structural and electrochemical properties, and develops an amperometric sensor for glucose. The synergistic effect of GNP and MWNTs films leads to better electrocatalytic ability and higher sensitivity to dissolved oxygen than GNP or MWNTs film alone. The good electrocatalytic ability makes the detection of glucose can be performed at a low reduction overpotential of dissolved oxygen, thus avoids the interference of electrochemically oxidable compounds. The multilayer structure helps to increase oxygen content around the electrode surface as well as its permeability, which results in high upper limit of glucose detection based on the consumption of dissolved oxygen, and thus increases the practicability of the proposed glucose biosensor.

5. Acknowledgements

This work was supported by the National Science Fund for Distinguished Young Scholars (20325518) and Creative Research Groups (20521503) and the Key Program from the National Natural Science Foundation of China (20535010).

6. References

[1] A. Henglein, *Chem. Rev.* **1989**, *89*, 1861.
[2] A. N. Shipway, M. Lahav, I. Willner, *Adv. Mater.* **2000**, *12*, 993.
[3] W. L. Cheng, S. J. Dong, E. K. Wang, *Langmuir* **2002**, *18*, 9947.
[4] S. Q. Liu, H. X. Ju, *Biosens. Bioelectron.* **2003**, *19*, 177.
[5] J. J. Feng, G. Zhao, J. J. Xu, H. Y. Chen, *Anal. Biochem*. **2005**, *342*, 280.
[6] C. R. Raj, A. I. Abdelrahman, T. Ohsaka, *Electrochem. Commun.* **2005**, *7*, 888.
[7] M. S. E. Deab, T. Ohsaka, *Electrochem. Commun.* **2002**, *4*, 288.
[8] M. Chirea, V. G. Morales, J. A. Manzanares, C. Pereira, R. Gulaboski, F. Silva, *J. Phys. Chem. B.* **2005**, *109*, 21808.
[9] W. Zhao, J. J. Xu, H. Y. Chen, *Front. Biosci.* **2005**, *10*, 1060.
[10] S. J. Tans, M. H. Devoret, H. J. Dai, A. Thess, R. E. Smalley, L. J. Geerllgs, C. Dekker, *Nature* **1997**, *386*, 474.
[11] E. W. Wong, P. E. Sheehan, C. M. Lieber, *Science* **1997**, *277*, 1971.
[12] M. Ouyang, J. L. Huang, C. M. Lieber, *Acc. Chem. Res.* **2002**, *35*, 1018.
[13] B. Munge, G. D. Liu, G. Collins, J. Wang, *Anal. Chem.* **2005**, *77*, 4662.
[14] S. G. Wang, R. L. Wang, P. J. Sellina, Q. Zhang, *Biochem. Biophys. Res. Co.* **2004**, *325*, 1433.
[15] Y. Liu, M. K. Wang, F. Zhao, Z. Xu, S. J. Dong, *Biosens. Bioelectron.* **2005**, *21*, 984.
[16] J. X. Wang, M. X. Li, Z. J. Shi, N. Q. Li, Z. N. Gu, *Anal. Chem.* **2002**, *74*, 1993.
[17] M. N. Zhang, Y. M. Yan, K. P. Gong, L. Q. Mao, Z. X. Guo, Y. Chen, *Langmuir* **2004**, *20*, 8781.
[18] A. Kongkanand, S. Kuwabata, G. Girishkumar, P. Kamat, *Langmuir* **2006**, *22*, 2392.
[19] S. Hrapovic, Y. L. Liu, K. B. Male, H. T. Luong, *Anal. Chem*. **2004**, *76*, 1083.
[20] Y. H. Lin, F. Lu, Y. Tu, Z. F. Ren, *Nano Lett*. **2004**, *4*, 191.
[21] M. N. Zhang, K. P. Gong, H. W. Zhang, L. Q. Mao, *Biosens. Bioelectron.* **2005**, *20*, 1270.
[22] M. L. Guo, J. H. Chen, J. Li, L. H. Nie, S. Z. Yao, *Electroanalysis* **2004**, *16*, 1992.
[23] X. L. Luo, J. J. Xu, J. L. Wang, H. Y. Chen, *Chem. Commun.* 2005, *16*, 2169.
[24] Y. C. Tsai, S. C. Li, J. M. Chen, *Langmuir* **2005**, *21*, 3653.
[25] J. Wang, M. Musameh, *Anal. Chem.* **2003**, *75*, 2075.
[26] S. H. Lim, J. Wei, J. Y. Lin, Q. T. Li, J. K. You, *Biosens. Bioelectron.* **2005**, *20*, 2341.
[27] Y. Q. Dai, K. K. Shiu, *Electroanalysis* **2004**, *16*, 1697.
[28] T. Rinken, T. Tenno, *Biosens. Bioelectron.* **2001**, *16*, 53.
[29] X. J. Wu, M. M. F. Choi, D. Xiao, *Analyst* **2000**, *125*,157.
[30] S. M. Reddya, P. Vadgama, *Anal. Chim. Acta* **2002**, *461*, 57.
[31] A. Maines, D. Ashworth, P. Vadgama, *Anal. Chim. Acta* **1996**, *333,* 223.
[32] A. E. Cass, G. G. Davis, G. D. Francis, H. A. Hill, W. J. Aston, I. J. Higgins, E. V. Plotkin, D. L. Scott, P. F. Turner, *Anal. Chem*. **1984**, *56*, 667.
[33] M. N. Zhang, L. Su, L. Q. Mao, *Carbon* **2006**, *44*, 276.
[34] S. H. Lim, J. Wei, J. Y. Lin, *Chem. Phys. Lett.* **2004**, *400*, 578.
[35] B. Kim, W. M. Sigmund, *Langmuir* **2004**, *20*, 8239.
[36] H. T. Zhao, H. X. Ju, *Anal. Biochem.* **2006**, *350*, 138.
[37] Y. Du, X. L. Luo, J. J. Xu, H. Y. Chen, *Bioelectrochemistry* **2006**, *71*, 44.
[38] Y. Xiao, H. X. Ju, H. Y. Chen, *Anal. Chim. Acta* **1999**, *391*, 73.
[39] S. T. Dubas, J. B. Schlenoff, *Langmuir* **2001**, *17*, 7725.
[40] A. J. Bard, L. R. Faulkner, *Electrochemical Methods-Fundamentals and Applications*, Wiley, New York **2000**.
[41] H. Tang, J. H. Chen, Z. P. Huang, D. Z. Wang, Z. F. Ren, L. H. Nie, Y. F. Kuang, S. Z. Yao, *Carbon* **2004**, *42,* 191.
[42] H. X. Ju, C. Z. Shen, *Electroanalysis* **2001**, *13*, 8.
[43] Y. Q. Dai, K. K. Shiu, *Electroanalysis* **2004**, *16*, 1697.
[44] T. Rinken, T. Tenno, *Biosens. Bioelectron.* **2001**, *16*, 53.
[45] B. Wang, B. Li, Q. Deng, S. Dong, *Anal. Chem.* **1998**, *70*, 3170.
[46] S. Sampath, O. Lev, *Anal. Chem*. **1996**, *68*, 2015.

